Local Structure Analysis of Lead Zinc Niobate-Barium Titanate Ceramic by X-Ray Absorption Spectroscopy and Density Functional Calculation *

Kanokwan Kanchiang[1**], Phakkhananan Pakawanit[2], Rattikorn Yimnirun[3]

[1]*Program in Applied Physics, Faculty of Science, Maejo University, Chiang Mai 50290, Thailand*
[2]*Synchrotron Light Research Institute, Ratchasima 30000, Thailand*
[3]*School of Physics, Institute of Science, and NANOTEC-SUT Center of Excellence on Advanced Functional Nanomaterials, Suranaree University of Technology, Nakhon Ratchasima 30000, Thailand*

(Received 23 February 2017)

The local structure of an alternative $Pb(Zn_{1/3}Nb_{2/3})O_3$-based perovskite ceramic is investigated. The $0.07BaTiO_3$-$0.93Pb(Zn_{1/3}Nb_{2/3})O_3$ ceramic is synthesized using a combination of $Zn_3Nb_2O_8$ B-site precursor and $BaTiO_3$ perovskite phase stabilizer. Then, x-ray absorption spectroscopy and density functional theory are employed to calculate the local structure configuration and formation energy of the prepared samples. Ba^{2+} is found to replace Pb^{2+} in A-site with Zn^{2+} occupying B-site in $Pb(Zn_{1/3}Nb_{2/3})O_3$, while in the neighboring structure, Ti^{4+} replaces Nb^{5+} in B-site with Pb^{2+} occupying A-site. With the substitution of $BaTiO_3$ in $Pb(Zn_{1/3}Nb_{2/3})O_3$, the bond length between Zn^{2+} and Pb^{2+} is longer than that of the typical perovskite phase of $Pb(Zn_{1/3}Nb_{2/3})O_3$. This indicates the key role of $BaTiO_3$ in decreasing the steric hindrance of Pb^{2+} lone pair, and the mutual interactions between Pb^{2+} lone pair and Zn^{2+} and the formation energy is seen to decrease. This finding of the formation energy and local structure configuration relationship can further extend a fundamental understanding of the role of $BaTiO_3$ in stabilizing the perovskite phase in $PbZn_{13}Nb_{23}O_3$-based materials, which in turn will lead to an improved preparation technique for desired electrical properties.

PACS: 61.05.cj, 61.43.Bn, 61.50.Ah DOI: 10.1088/0256-307X/34/8/086102

$Pb(Zn_{1/3}Nb_{2/3})O_3$ (PZN)-based ceramics are one of the most widely used as relaxor ferroelectric materials with perovskite structures due to their excellent dielectric, piezoelectric and electrostrictive properties.[1–3] However, the PZN ceramic was found to be more difficult to prepare in the pure perovskite phase by conventional mixed oxide processing.[4,5] This is due to the fact that the PZN ceramic has low tolerance factor, small electronegativity difference between the cations, and the pyrochlore phase appears to be more thermodynamically stable than the perovskite phase.[6,7] Therefore, it is of great interest to investigate the perovskite instability of PZN ceramics, especially from the local structural information at microscopic viewpoint. Note that if the knowledge of how to enhance the stabilities of the perovskite phase is comprehensively obtained, one can therefore design an applicable processing route to enhance the perovskite phase by avoiding the pyrochlore phase. The previous work employed a combination of the experimental x-ray absorption spectroscopy analysis and density functional theory (DFT) calculation to give more insight into the local structure configuration and the formation behavior of lead zinc niobateceramic.[8] The result showed that the preparation method to obtain lead zinc niobate (PZN) ceramic in perovskite phase should focus on canceling or decreasing the steric hindrance of Pb^{2+} lone pairs and the mutual interaction between Pb^{2+} lone pairs and Zn^{2+} cations. For instance, PZN can be synthesized under high pressure (from 15 to 35 GPa) at high temperature (about 1100℃ to 1200℃).[9,10] Moreover, PZN in the perovskite phase can also be stabilized by partial substitution on *A*- or *B*-site cations using, e.g., $BaTiO_3$, $SrTiO_3$, $PbTiO_3$ and $PbZrO_3$ as matrixes.[11,12] The substituted *A*-site cations with spherical shape replace Pb^{2+} cations and the substituted *B*-site cations with high valence replace Zn^{2+} cations, which can help decrease the steric hindrance of Pb^{2+} lone pair and the mutual interaction between Pb^{2+} lone pairs and Zn^{2+} cations.

As mentioned above, to synthesize low-cost perovskite PZN, Furukawa *et al.*[13] reported the successful fabrication of pure perovskite PZN using 15 mol% $BaTiO_3$ additive. Later, it was confirmed by Halliyal *et al.*[14] that only 7 mol $BaTiO_3$ additive is sufficient to suppress the pyrochlore formation in the fabrication of perovskite PZN ceramics. Interestingly, no systematic study on the fabrication of perovskite $0.07BaTiO_3$-$0.93PbZn_{13}Nb_{23}O_3$ (0.07BT-0.93PZN) ceramic using a combination of *B*-site precursor $Zn_3Nb_2O_8$ and reactive sintering process has been carried out. Thus in this work, a perovskite solid solution having a composition 0.07BT-0.93PZN ceramic is prepared with the $Zn_3Nb_2O_8$ *B*-site precursor technique, instead of using a well-known precursor of columbite type $ZnNb_2O_6$, and it is then fired under various conditions through a reactive sintering process. Then, a combination of x-ray absorption spectroscopy analysis and DFT calculation is used to in-

*Supported by the Thailand Research Fund under Grant No TRG5880097.
**Corresponding author. Email: kanokwan_physics@hotmail.com
© 2017 Chinese Physical Society and IOP Publishing Ltd

vestigate the effect of BT on 0.07BT-0.93PZN structure configuration. This fundamental understanding of the total energy and local structure relationship can be further extended to improve the preparation technique of perovskite lead zinc niobate ceramics that yield the desired electrical properties.

The powerful analytical technique to determine local structure configuration around the interesting atom in the sample is the combination of x-ray absorption spectroscopy and DFT. In the x-ray absorption spectroscopy, the amount of the x-ray photon absorbed by the interesting atom was measured as a function of x-ray energy. The x-ray absorption spectrum can be divided into two regions according to the x-ray photon energies. The low energy region covers photon energy up to about 50 eV above the absorption edge, i.e., the x-ray absorption near edge structure (XANES). The qualitative picture of atomic environment around the interesting atom was presented by the feature peaks of the XANES spectrum. The high energy region covers photon energy up to about 1000 eV above the absorption edge, i.e., the extended x-ray absorption fine structure (EXAFS). The quantitative approximate radial distribution of neighboring atoms around the interesting atom was presented by the distinctive peaks in the Fourier transform of the EXAFS spectrum.[15] From the information of microscopic local structure configuration, the DFT is used to calculate total energies and atomic interactions along the chemical reaction to find the effect of local structure configuration changing to the formation energy, which is the cause of perovskite stability.

The lead zinc niobate-barium titanate ($0.07BaTiO_3$-$0.93PbZn_{13}Nb_{23}O_3$) ceramic was synthesized with the combination of the $Zn_3Nb_2O_8$ B-site precursor and the $BaTiO_3$ perovskite phase stabilizer. The x-ray diffraction pattern was measured using a Philips PW 1729 diffractometer with Ni-filtered Cu K_α radiation at room temperature. The x-ray diffraction pattern indicates the formation of $0.07BaTiO_3$-$0.93PbZn_{13}Nb_{23}O_3$ in the rhombohedral phase with cell parameter $a = 4.063$ Å and $\alpha = 89.96°$ in space group $R3m$ (No. 160), matching with the JCPDS file number 22–663.[16] The Zn K-edge of both XANES and EXAFS spectra were measured at Beamline 5, Synchrotron Light Research Institute, Thailand, with the storage ring running at energy of 12 GeV and currents ranging from 120 to 80 mA. These spectra were recorded in the fluorescence mode with 5 Ge detectors at room temperature. These multiple scanned spectra were recorded and merged after performing an absorption edge energy calibration. The merged spectrum was subtracted with the pre-edge line and post-edge line and later normalized an absorption edge jump height to unity.[17] These normalized spectra were performed using the IFEFFIT package.[18,19]

After that, the atomic configuration of $0.07BaTiO_3$-$0.93PbZn_{13}Nb_{23}O_3$ ceramic was investigated. All possible atomic positions in 0.07BT-0.93PZN structural models were generated with the typical perovskite $PbZn_{13}Nb_{23}O_3$ host structure in space group $R3m$ (No. 160)[20] and optimized using DFT. In the typical perovskite structure, it is known that $BaTiO_3$ has the Ba atom on A-site and the Ti atom on B-site. However, compared to $0.07BaTiO_3$-$0.93PbZn_{13}Nb_{23}O_3$, it is possible that the Ba atom A-site and the Ti atom on B-site would be replaced in the structure of $PbZn_{13}Nb_{23}O_3$. The atomic positions of $0.07BaTiO_3$-$0.93PbZn_{13}Nb_{23}O_3$ ceramic were obtained by the comparison between measured and simulated XANES spectra with all possible structural models, and then the radial distribution around the Zn atom was extracted from the EXAFS spectrum analysis.

To identify the atomic configuration of the perovskite $0.07BaTiO_3$-$0.93PbZn_{13}Nb_{23}O_3$ or 0.07BT-0.93PZN ceramic, the structural models of $BaTiO_3$ substituting in perovskite $PbZn_{13}Nb_{23}O_3$ were created and optimized using DFT. The starting structural models are obtained from the rhombohedral phase of typical perovskite $PbZn_{13}Nb_{23}O_3$.[20] In the perovskite $BaTiO_3$ structure, the Ba atom occupies A-site and the Ti atom occupies B-site, thus it is highly possible that the Ba atom on A-site is substituted and the Ti atom on B-site is substituted to form the perovskite $PbZn_{13}Nb_{23}O_3$ structure. The structural model consisting of 3×3×3 supercell of typical $PbZn_{13}Nb_{23}O_3$ perovskite phase was generated with all possible sites of $BaTiO_3$ in $0.07BaTiO_3$-$0.93PbZn_{13}Nb_{23}O_3$ as follows: (1) In the PZN structure, the Pb atom is replaced by Ba atom in A-site, and the Zn atom occupies B-site. In the neighboring structure, the Pb atom occupies A-site, and the Nb atom occupies B-site (model I). (2) In the PZN structure, the Pb atom is replaced by the Ba atom in A-site, and the Zn atom occupies B-site. In the neighboring structure, the Pb atom occupies A-site, and the Nb atom is replaced by the Ti atom in B-site, resulting in oxygen vacancy for local charge balancing (model Ⅱ). (3) The Ba and Ti atoms are not replaced in the PZN structure (model Ⅲ).

In the structural relaxation, the exchange correlation functional was used with the generalized gradient approximation (GGA).[21] Only valence electrons were considered exactly while core electronic states were represented via ultrasoft pseudopotentials. The plane wave cutoff energy was set to 3 eV and the Monkhorst–Pack grid of 4×4×4 points exists in the Brillouin zone. The atomic positions of all atoms are allowed to vary to minimize the total energy and converge when the difference in total energies between the successive iterations is less than 10^{-5} eV, and the lattice parameters were fixed to the x-ray diffraction experimental data. The structural relaxation results of models I, Ⅱ and Ⅲ

are presented in Fig. 1.

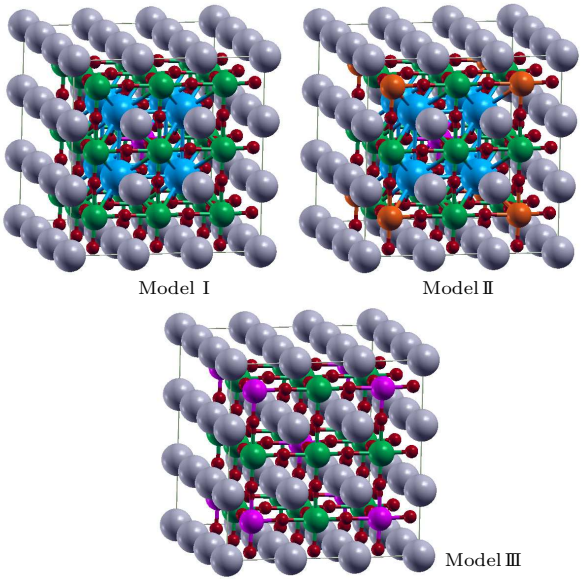

Fig. 1. The structural relaxation results of models I, Ⅱ and Ⅲ, where the gray ball is the Pb atom, the pink ball is the Zn atom, the green ball is the Nb atom, the red ball is the O atom, the blue ball is the Ba atom, and the orange ball is the Ti atom.

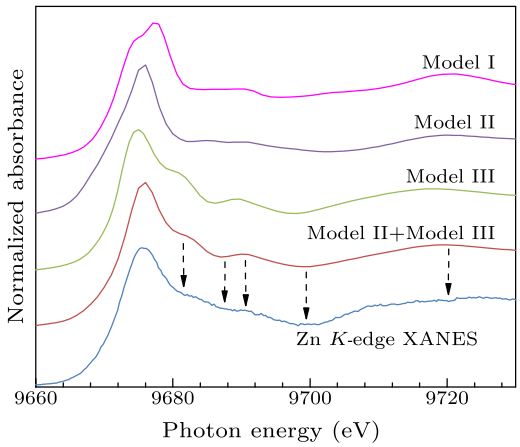

Fig. 2. The comparison between the measured Zn K-edge XANES spectrum in 0.07BT-0.93PZN ceramic and the simulated Zn K-edge XANES spectra of models I, Ⅱ and Ⅲ.

After structural relaxation, Zn K-edge XANES spectra were simulated with structural models of the Ba atom substituted on A-site and the Ti atom substituted on B-site in the perovskite PZN structure using the FEFF code, which employs a full-multiple scattering approach based on self-consistent overlapping muffin-tin potentials. The self-consistent calculations were performed in a cluster with a radius of 47 Å (about 45 atoms) away from the absorbing Zn atom. The full multiple scattering calculations included all possible paths with a cluster with a radius of 71 Å (about 119 atoms) away from the absorbing Zn atom. The results of simulated Zn K-edge XANES spectra of models I, Ⅱ and Ⅲ are presented in Fig. 2. As can be seen, the absorbance features are varied, depending on the different atomic environment geometries around the Zn atom in pure or partial replacing by the Ba atom on A-site and the Ti atom on B-site in the PZN perovskite structure. It is found that the combination of absorbance features of the simulated Zn K-edge XANES spectra of the Zn atom in models Ⅱ and Ⅲ is overall consistent with the measured spectrum. The results clearly indicate the qualitative atomic configuration of 0.07BT-0.93PZN as follows: (1) The Zn atom occupies A-site and the Pb atom occupies B-site, while in the neighboring structure, the Pb atom occupies A-site and the Nb atom occupies B-site. (2) The Zn atom occupies A-site and the Ba atom occupies B-site, while in the neighboring structure, the Pb atom occupies A-site, the Ti and Nb atoms occupy B-site.

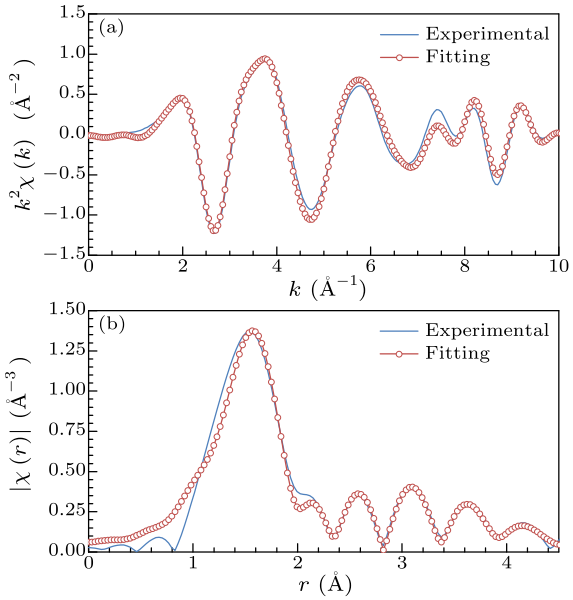

Fig. 3. The EXAFS oscillation and fitting results in k-space (top) and R-space (bottom) of 0.07BT-0.93PZN. The fitting was performed in the k range from 1.5 to 10.0 Å^{-1} and in the R range from 0.8 to 4.4 Å.

The quantitative local structural information around the Zn atom, including the average coordination number N, the average distance R, and the mean square variations σ^2) of neighboring atoms, was obtained by the Zn K-edge EXAFS analysis to find the best modeled EXAFS function that fits well with the measured EXAFS spectrum. The modeled EXAFS function was constructed from a set of the possible scattering paths of photoelectron scattered from the distribution of neighboring atoms using the FEFF6 code. The common shift of the energy at the origin (E_0) was allowed to vary. The amplitude reduction factor S_0^2 was fixed at 0.94. The atomic species of neighbors were recognized in the fit from their specific scattering factors $F_j(k)$ and phase shifts $\delta_j(k)$.

The fitting was performed in the k range from 1.5 to 10.0 Å^{-1} and in the R range from 0.8 to 4.4 Å. The fitting is concluded when the R factor is smaller than or equal to a threshold (0.01 in this case) and the number of variables ($N = 15$) is less than that of the independent points $N_{\rm idp} = 17$, as shown in Fig. 3. The fitting results are listed in Table 1. It is found that the approximate bond length between Zn^{2+} and Pb^{2+} is about 3.4094 Å, which is longer than that of typical perovskite PZN (3.3642 Å).

Table 1. The structural parameters of 0.07BT-0.93PZN obtained from the EXAFS analysis, where N is the coordination number, R is the average distance, and σ^2 is the mean square variations of the neighboring atoms.

Path	N	R (Å)	σ^2 (Å^{-1})	R-factor
Zn–O1	3	2.0724	0.0078	0.0108
Zn–O1	3	2.8238	0.0894	
Zn–Pb1	1	2.9139	0.0126	
Zn–Pb2	3	3.2127	0.0066	
Zn–Pb3	3	3.4684	0.0081	
Zn–Pb4	1	4.3124	0.0010	

Additionally, to investigate the barium titanate role to perovskite phase formation of barium titanate lead zinc niobate ceramic, the total energy along reaction paths from the precursors $Zn_3Nb_2O_8$ with space group $C2c$ (No. 15),[22] Nb_2O_5 with space group $Pbam$ (No. 55)[23] and PbO with space group $Pbcm$ (No. 57)[24] to perovskite $PbZn_{13}Nb_{23}O_3$ phase with space group $R3m$ (No. 160)[20] and from the precursors $Zn_3Nb_2O_8$ with space group $C2c$ (No. 15),[22]) Nb_2O_5 with space group $Pbam$ (No. 55),[23] PbO with space group $Pbcm$ (No. 57),[24] $BaTiO_3$ with space group $R3m$ (No. 160)[25] to perovskite $0.07BaTiO_3$-$0.93PbZn_{13}Nb_{23}O_3$ phase with space group $R3m$ (No. 160) was calculated using the following chemical reactions: $19Zn_3Nb_2O_8+29Nb_2O_5+PbO \rightarrow PbZn_{13}Nb_{23}O_3$, and $0313Zn_3Nb_2O_8+0623Nb_2O_5+0.93PbO+0.07BaTiO_3 \rightarrow 086PbZn_{13}Nb_{23}O_3+0.07BaZn_{13}Nb_{23}O_3+0.07PbTiO_3$.

From the DFT calculations of both the reaction paths, the formation energy of the PZN perovskite phase (−0.0119 eV) is about 5.7×10^{-3} eV noticeably higher than that of the 0.93PZN-0.07BT perovskite phase (−0.0176 eV). This is due to the fact that the Pb^{2+} cation is not spherically arisen from the presence of the $6s^2$ lone pair. The steric hindrance of Pb^{2+} lone pairs and the mutual interactions between Pb^{2+} lone pairs and Zn^{2+} cations are therefore the impediment factors in perovskite phase formation. The substitution of spherical Ba^{2+} cation in the position of Pb^{2+} cation then decreases the mutual interaction between Pb^{2+} lone pairs and Zn^{2+} cations. Nevertheless, the substitution of smaller-ionic-radius Ti^{4+} cations in the position of Zn^{2+} and Nb^{5+} cations can decrease the bond length between Pb^{2+} and Zn^{2+} and can reduce the mutual interaction between Pb^{2+} lone pairs and Zn^{2+} cations. Therefore, the lower formation energy is required to compensate for these remaining mutual interactions and 0.07BT-0.93PZN can form in the perovskite phase.

In summary, the local structure configuration of the perovskite $0.07BaTiO_3$-$0.93PbZn_{13}Nb_{23}O_3$ ceramic has been investigated by employing the combination of x-ray absorption spectroscopy and DFT analysis. The result shows that Ba^{2+} replaces Pb^{2+} in A-site with Zn^{2+} occupying B-site in $PbZn_{13}Nb_{23}O_3$, while in the neighboring structure, Ti^{4+} replaces Nb^{5+} in B-site with Pb^{2+} occupying A-site. From the substitutions of $BaTiO_3$ in $PbZn_{13}Nb_{23}O_3$, the bond length between Zn^{2+} and Pb^{2+} is longer than that of the typical perovskite phase of $PbZn_{13}Nb_{23}O_3$, which indicates the main role of $BaTiO_3$ in decreasing the steric hindrance of Pb^{2+} lone pairs and the mutual interactions between Pb^{2+} lone pairs and Zn^{2+}.

References

[1] Zeng X, Ding A L, Liu T, Deng G C and Zheng X S 2005 *Phys. Status Solidi* A **202** 1842
[2] Srimathy B, Jayavel R, Ganesamoorthy S, Bhaumik I, Karnal A K, Natarajan V, Varadarajan E and Kumar J 2012 *Cryst. Res. Technol.* **47** 523
[3] Shi L, Liao Q W, Zhang B P, Zhang J Y and Guo D 2014 *Mater. Lett.* **114** 100
[4] Fujiu T, Tanaka A and Takenaka T 1991 *Jpn. J. Appl. Phys.* **30** L298
[5] Lee W S, Isobe T and Senna M 2002 *Adv. Powder Technol.* **13** 43
[6] Ohwa H, Iwata M, Yasuda N and Ishibashi Y 1998 *Jpn. J. Appl. Phys.* **37** 5410
[7] Tomeno I, Shimanuki S, Tsunoda Y and Ishii Y 2001 *J. Phys. Soc. Phys. Jpn.* **70** 1444
[8] Kanchiang K, Pramchu S, Yimnirun R, Pakawanit P, Ananta S and Laosiritaworn Y 2013 *J. Appl. Phys.* **114** 064103
[9] Matsuo Y, Sasaki H, Hayakawa S, Kanamaru F and Koizumi M 1969 *J. Am. Ceram. Soc.* **52** 516
[10] Ravindranathan P, Srikanth V, Komarneni S and Bhalla A S 1996 *Ferroelectrics* **188** 135
[11] Ahn B Y and Kim N K 2004 *J. Am. Ceram. Soc.* **83** 1720
[12] Yun S and Wang X 2006 *Mater. Chem. Phys.* **98** 62
[13] Furukawa O, Yamashita Y, Harata M, Takahashi T and Inagaki K 1985 *Jpn. J. Appl. Phys.* **24** 96
[14] Halliyal A, Kumar U, Newnham R E and Cross L E 1987 *Am. Ceram. Soc. Bull.* **66** 671
[15] Aksenov V L, Yu A, Purans J and Tyutyunnikov S I 2001 *Phys. Part. Nuclei* **32** 1
[16] Pakawanit P, Ngamjarurojana A, Prasatkhetragarn A and Ananta S 2013 *Ferroelectrics* **454** 84
[17] Weng T C, Waldo G S and Penner-Hahn J E 2005 *J. Synchrotron Rad.* **12** 506
[18] Ravel B and Newville M 2005 *Phys. Scr.* **115** 1007
[19] Ravel B and Newville M 2005 *J. Synchrotron Rad.* **12** 537
[20] Kisi E H, Forrester J S and Knight K S 2006 *Acta Crystallogr.* C **62** i46
[21] Hua X, Chen X and Goddard W A 1997 *Phys. Rev.* B **55** 16103
[22] Isobe M, Marumo F, Iwai S I and Kondo Y 1974 *Bull. Tokyo Inst. Technol.* **120** 1
[23] Kato K and Tamura S 1975 *Acta Crystallogr.* B **31** 673
[24] Hill R 1985 *Acta Crystallogr.* C **41** 1281
[25] Kwei G H, Lawson A C, Billinge S J L and Cheong S W 1993 *J. Phys. Chem.* A **97** 2368